Adsorption of Semiflexible Polyelectrolytes on Charged Planar Surfaces: Charge Compensation, Charge Reversal, and Multilayer Formation

Roland R. Netz*,† and Jean-François Joanny‡

Max-Planck-Institut für Kolloid- und Grenzflächenforschung, Am Mühlenberg, 14424 Potsdam, Germany, and Institut Charles Sadron, 6 rue Boussingault, 67083 Strasbourg, France

Received February 23, 1999; Revised Manuscript Received July 26, 1999

ABSTRACT: We study theoretically the adsorption of semiflexible charged polymers on an oppositely charged flat substrate. We restrict ourselves to polymers with relatively high line charge density τ and bare bending stiffness l_0, such as DNA or fully charged synthetic polyelectrolytes, for which the condition $\tau^2 l_B l_0 > 1$ (with $l_B = e^2/4\pi\epsilon k_B T$ denoting the Bjerrum length) is satisfied. In this case the effective bending rigidity (which includes chain stiffening due to electrostatic monomer−monomer repulsion) is always larger than the screening length, and we obtain very thin adsorption layers, where the polymers essentially lie flat on the surface and can be considered as a two-dimensional layer. We distinguish different adsorbed phases, including a two-dimensional lamellar phase where the polymers run parallel and do not overlap and a disordered phase where the polymers form a random network with multiple crossings. By explicitly including lateral correlations within the adsorbed layer, we find a regime of strong charge reversal, where the adsorbed phase exhibits a much higher surface charge density than the substrate and thus reverses the charge of the substrate by a factor much larger than unity. This charge-reversed regime is characterized by a typical distance between polymers larger than the screening length. We explicitly take image charge effects due to a dielectric jump at the substrate surface and the impenetrability of the substrate for salt ions into account. These effects lead to an increase of the electrostatic persistence length close to the substrate and inhibit adsorption for strongly charged polymers and low-dielectric substrates. At the end, we present some scaling arguments for the formation of charge-oscillating multilayers.

I. Introduction

Polyelectrolytes are polymers built of monomers which (upon dissolution in water) acquire an electric charge. Because of the entropy associated with counterion release, they are soluble in water, which explains their widespread use and applications.[1−3] The long-range character of the electrostatic interactions gives polyelectrolytes very specific properties which are only partially understood from the theoretical point of view.[4] Experimentally, the adsorption of charged polymers on charged or neutral substrate has been characterized as a function of the polymer charge, chemical composition of the substrate, and pH and ionic strength of the solution.[5−7] The adsorption on charged membranes[8−11] or monolayers[12,13] allows in addition to control the substrate charge density but also leads to additional effects which have to do with the fluid nature of the substrate[14] and the possibility of three-dimensional ordered structures.[15] Repeated adsorption of anionic and cationic polyelectrolytes[16] can lead to well-characterized multilayers.[17−19] Theoretically, the adsorption of polyelectrolytes on charged surfaces poses a much more complicated problem than the corresponding behavior of neutral polymers. The adsorption process results from a subtle balance between electrostatic repulsions between charged monomers, which leads, inter alia, to chain stiffening, and electrostatic attractions between the substrate and the polymer chain. Early theoretical studies employed numerical mean-field methods, which use a discrete lattice model for the polymer.[20−22] The same problem was also treated with the uniform expansion method[23] and various continuous mean-field theories.[24−27] In all these works, the lateral polymer distribution is treated as homogeneous.

In this paper we treat the adsorption of semiflexible polyelectrolytes on an oppositely charged planar surface, allowing for laterally ordered adsorbed phases and thereby including lateral correlations. The attractive electrostatic interactions between the polymer and the substrate are changed by varying the polymer linear charge density, the surface-charge density of the substrate, and the ionic strength of the solution. Image charge effects, which arise because the substrate has in general a dielectric constant different from that of the polymer solution, turn out to play an important role, and for low-dielectric substrates they induce desorption if the polymer linear charge density is too high. The intrinsic stiffness of the chain is another parameter that is varied. We treat all electrostatic interactions on the Debye−Hückel level, but as we show below, there is a large range of salt concentrations for strongly charged polymers where this is a valid approximation. The entropy of counterion release (which has been shown to favor complexation[28]) is therefore only captured on a linear level. We first investigate the adsorption of a single semiflexible polymer (section II.A). If the screening length is smaller than the effective persistence length of the polymer (which is the limit we always consider in this paper), we find that there is a maximal layer thickness which can be reached of the order of the screening length. The polymer thus forms, in general, a flat adsorption layer without loops. In section II.C we take into account many-chain effects by considering

† Max-Planck-Institut.
‡ Institut Charles Sadron.

10.1021/ma990263h CCC: $18.00
Published on Web 12/04/1999

different adsorbed surface phases, including a lamellar phase with predominantly parallel polymers and a disordered phase with many chain crossings. The general trend that comes out of the calculation is that, for an adsorbed phase with typical distances between neighboring polymers smaller than the screening length, we can neglect lateral correlations and instead represent the adsorbed phase by a homogeneous, smeared-out phase, which is equivalent to a mean-field approximation. In this case there is only *marginal charge reversal* (up to 14%). If, on the other hand, the lamellar spacing becomes larger than the screening length, we find what we call *strong charge reversal*, where the adsorbed surface charge density can be many times the substrate charge density. In section III we present a typical phase diagram, featuring the lamellar, strongly charge-reversed phase and a charge-compensated adsorbed phase. Recent interest in the effect of charge reversal has been stirred by new techniques of multilayer formation.[17,18] For thin adsorbed layers, strong charge reversal is a prerequisite for the adsorption of a second layer of oppositely charged polymers. However, charge reversal is also important for controlled flocculation of colloidal suspensions. In section IV, we present some rough scaling arguments for the formation of multilayers. We first show that multilayers cannot form if the typical mesh size within the multilayer is smaller than the screening length. For the opposite case, we obtain a formula which gives the surface charge density of the adsorbed layer as a function of the surface charge density of the previous polymer layer. This formula acts as a nonlinear map and shows a stable fixed point at a polymer mesh size corresponding to the persistence length. The last section presents concluding remarks and raises some open issues.

II. Adsorption Model

A. Adsorption of a Single Semiflexible Polymer. In this section we discuss on a scaling level the adsorption behavior of a single semiflexible charged chain on an oppositely charged plane, which is a slight modification of the analogous results obtained for flexible polymers.[29] As is discussed in details in Appendix A, a charged polymer (with τ unit charges per unit length) is subject to the electrostatic potential created by the homogeneous charge distribution on the substrate surface (carrying σ unit charges per unit area), eq A6, which is attractive for an oppositely charged substrate. We consider the potential in eq A6 as the driving force for the adsorption. There are also more complex interactions due to the dielectric discontinuity at the substrate surface and due to the impenetrability of the substrate for salt ions. The resulting interaction is repulsive for a substrate dielectric constant ϵ' smaller than the solvent dielectric constant ϵ and is explicitly displayed for $\epsilon'/\epsilon = 0$ in eq A9 and for $\epsilon'/\epsilon = 1$ in eq A10 (for the case of adsorption on a metallic substrate, characterized by $\epsilon'/\epsilon = \infty$, there is also the possibility of an attractive self-energy which could induce polyelectrolyte adsorption on noncharged substrates or on substrates bearing charges of the same sign as the polyelectrolyte; this case we do not explicitly pursue in this paper).

In the following we concentrate on substrates with a dielectric constant much lower than that of water, in which case eq A9 is a good approximation. As it turns out later on, the adsorbed layers are always thinner than the screening length; the repulsion due to image charge effects per unit polymer length can thus be written as

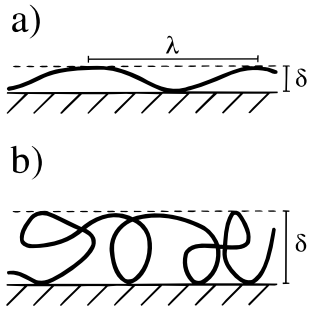

Figure 1. (a) Schematic picture of the adsorbed polymer layer when the effective persistence length is larger than the layer thickness, $l_{eff} > \delta$. The distance between two collisions of the polymer with the substrate, the so-called deflection length, scales as $\lambda \sim \delta^{2/3} l_{eff}^{1/3}$. (b) Adsorbed layer for the case when the layer thickness is larger than the persistence length, in which case the polymer forms a random coil with many loops and a description in terms of a flexible polymer model becomes appropriate. For a screening length smaller than the polymer persistence length, we only find flat adsorbed layers as depicted in (a).

$$f_{im} = l_B \tau^2 K_0[2\kappa\delta] \simeq -l_B \tau^2 \ln(2\kappa\delta) \qquad (1)$$

where δ denotes the width or typical distance of the polymer from the substrate surface and $l_B = e^2/4\pi\epsilon k_B T$ the Bjerrum length. Note that in this paper all interactions and free energies are measured in units of the thermal energy $k_B T$. Using the DH electrostatic potential distribution of a homogeneously charged plane as given in eq A6, $V_{plane}(z) = 4\pi l_B \sigma \kappa^{-1} e^{-\kappa z}$, and assuming that the adsorbed polymer layer has a homogeneous vertical density distribution over its entire width δ, the electrostatic attraction per polymer unit length can be written as

$$f_{att} = -\frac{4\pi l_B \sigma\tau}{\kappa} \int_0^\delta \frac{dz}{\delta} e^{-\kappa z} = -\frac{4\pi l_B \sigma\tau (1 - e^{-\delta\kappa})}{\delta\kappa^2} \qquad (2)$$

Due to the confinement in the adsorbed state, the polymer feels an entropic repulsion. If the layer thickness δ is much smaller than the effective persistence length of the polymer, l_{eff}, as depicted in Figure 1a, the polymer does on average suffer one collision per deflection length λ. As shown by Odijk, the deflection length scales as $\lambda \sim \delta^{2/3} l_{eff}^{1/3}$ and is thus larger than the layer thickness δ but smaller than the persistence length l_{eff}.[30] The entropic repulsion follows in a simple manner from the deflection length by assuming that the polymer loses roughly one $k_B T$ per deflection. If on the other hand the layer thickness is larger than the persistence length, as shown in Figure 1b, the polymer forms a random coil with many loops within the adsorbed layer. For a contour length smaller than $L \sim \delta^2/l_{eff}$ the polymer obeys Gaussian statistics; beyond this length scale the polymer decorrelates into blobs with an entropic cost of one $k_B T$ per blob. The entropic repulsion per polymer unit length is thus[30]

$$f_{rep} \sim \begin{cases} 1/\delta^{2/3} l_{eff}^{1/3} \ln(l_{eff}/\delta) & \text{for } \delta \ll l_{eff} \\ l_{eff}/\delta^2 & \text{for } \delta \gg l_{eff} \end{cases} \qquad (3)$$

where the logarithmic cofactor (which is rather unimportant for our scaling arguments) arises because

deflected stiff polymer segments show large angular correlations. As shown in Appendix B, there is a modification of the electrostatic stiffening of a charged polymer close to a solid substrate which takes into account the dielectric jump and the impenetrability of the wall for salt ions. As a result, the electrostatic persistence length is increased by a factor of 2 and contains a logarithmic dependence on the screening length. In Appendix C, we discuss in details how the effective persistence length l_{eff} depends on the screening length and the line charge density; in essence, one has to keep in mind that the effective persistence length is for a wide range of parameters larger than the bare persistence length due to electrostatic stiffening effects. Let us first calculate the layer thickness and neglect for the moment image-charge effects; we will later take image charge effects into account. The equilibrium layer thickness follows from a minimization of the sum of eqs 2 and 3. For large salt concentrations (or rather stiff polymers) and small layer thickness, $\delta < \kappa^{-1} < l_{\mathrm{eff}}$, we obtain

$$\delta \sim \left(\frac{\ln[l_{\mathrm{B}}\sigma\tau l_{\mathrm{eff}}^{2}]}{l_{\mathrm{B}}\sigma\tau l_{\mathrm{eff}}^{1/3}}\right)^{3/5} \tag{4}$$

For larger layer thickness, $\kappa^{-1} < \delta < l_{\mathrm{eff}}$, the attraction in eq 2 goes like $f_{\mathrm{att}} \sim -\delta^{-1}$ and the repulsion in eq 3 as $f_{\mathrm{rep}} \sim \delta^{-2/3}$. It is clear that there is no stable minimum for this range of layer thicknesses. At a layer thickness corresponding to the screening length one therefore encounters for stiff polymers (characterized by $\kappa^{-1} < l_{\mathrm{eff}}$) a discontinuity at which the polymer desorbs abruptly. This is in accord with previous transfer-matrix calculations for semiflexible polymer bound by short-ranged (square-well) potentials.[31−33] It should be clear that for long enough polymers, the desorption transition is—at least in the asymptotic limit—continuous. But the crossover from discontinuous to continuous can be very slow and, for stiff polymers, unobservable experimentally. Setting $\delta \sim \kappa^{-1}$ in eq 4, we obtain as the adsorption threshold (for $\kappa l_{\mathrm{eff}} > 1$)

$$\sigma_{\mathrm{ads}} \sim \frac{\kappa^{5/3}}{\tau l_{\mathrm{eff}}^{1/3} l_{\mathrm{B}}} \tag{5}$$

For $\sigma > \sigma_{\mathrm{ads}}$ the polymer is adsorbed and localized over a vertical width smaller than the screening length (and with the condition $l_{\mathrm{eff}} > \kappa^{-1}$ also smaller than the persistence length). At $\sigma \sim \sigma_{\mathrm{ads}}$ the polymer discontinuously desorbs. Let us now consider the limit $l_{\mathrm{eff}} < \kappa^{-1}$. From eq 4 we gather that the layer thickness is of the order of the persistence length for $l_{\mathrm{B}}\sigma\tau l_{\mathrm{eff}}^{2} \sim 1$, at which point the assumptions made in deriving eq 4 break down. If the layer thickness is larger than the persistence length but smaller than the screening length, $l_{\mathrm{eff}} < \delta < \kappa^{-1}$, the prediction for the layer thickness (obtained from a minimization of the sum of eqs 2 and 3) becomes

$$\delta \sim \left(\frac{l_{\mathrm{eff}}}{l_{\mathrm{B}}\sigma\tau}\right)^{1/3} \tag{6}$$

From this expression we see that the layer thickness becomes of the order of the screening length for

$$\sigma_{\mathrm{ads}} \sim \frac{l_{\mathrm{eff}}\kappa^{3}}{\tau l_{\mathrm{B}}} \tag{7}$$

which in fact denotes the location of a continuous adsorption transition at which the layer width grows to infinity.[34] The scaling results for the adsorption behavior of a flexible polymer, eqs 6 and 7, are in agreement with previous results.[23] Balancing now the image-charge repulsion eq 1 with the attraction eq 2, we obtain for the equilibrium layer thickness

$$\delta \sim \frac{\tau}{\sigma} \tag{8}$$

The layer thickness becomes of the order of the screening length for a substrate charge

$$\sigma_{\mathrm{ads}} \sim \tau\kappa \tag{9}$$

which denotes the desorption transition due to image-charge effects.

In the following, we only consider strongly charged polymers, defined by the condition $\tau(l_{\mathrm{B}}/l_0)^{1/2} > 1$. The adsorption transitions are defined by eqs 5 and 9, and the adsorption mechanism via the formation of a thick layer of loops, determined by the adsorption threshold eq 7, is never observed. The repulsive forces are dominated by image charge effects for $\sigma < \sigma_{\mathrm{im}}$ with

$$\sigma_{\mathrm{im}} \sim l_{\mathrm{B}}^{3/2} l_{\mathrm{eff}}^{1/2} \tau^{4} \tag{10}$$

as follows by comparison of the layer thicknesses in eqs 4 and 8. The higher the line charge of the polymer, the higher this crossover substrate charge density.

One can also show (taking into account that the persistence length l_{eff} must be calculated at a length scale given by the deflection length) that the effective persistence length at the desorption threshold is the bare persistence length l_0.

B. Debye−Hückel Approximation. In this paper we confine ourselves to the Debye−Hückel regime, where the electrostatic potential acting on an elementary charge is smaller than $k_{\mathrm{B}}T$ everywhere, including the substrate surface and the surface of the polymer chain. In this regime, the superposition principle for the electrostatic potential is valid, and therefore, all electrostatic interactions can be calculated by pairwise summation of the screened Coulomb potential $\tilde{\nu}_{\mathrm{DH}}(\mathbf{r}, \mathbf{r}')$ as defined in eq A2. If the electrostatic potential becomes larger than $k_{\mathrm{B}}T$ anywhere in the system, one in principle has to solve the full nonlinear Poisson−Boltzmann equation, which is a formidable task in all but the simplest geometries. We therefore exclude strongly charged surfaces and strongly charged polymers, for the merit of a consistent and accurate treatment of electrostatic interactions. As we show in this section, and contrary to what seems to be commonly believed, there is a wide range of salt concentrations where the Debye−Hückel approximation is valid, even for strongly charged polymers which are above the so-called Manning threshold (defined by $\tau l_{\mathrm{B}} > 1$).

For a charged planar surface of uniform charge density σ, the reduced electrostatic potential at the substrate (relative to the bulk potential infinitely far away from the surface) is within DH theory given by $V_{\mathrm{plane}}(z = 0) = 4\pi l_{\mathrm{B}}\sigma\kappa^{-1}$ (compare eq A6). The limit of applicability of DH theory, defined by $V_{\mathrm{plane}}(z = 0) < 1$,

is therefore (neglecting constants of order unity) given by

$$\sigma < \frac{\kappa}{l_B} \tag{11}$$

For a cylinder of radius D and surface charge density $\tau/(2\pi D)$ the surface potential is given by eq A12 and reads $V_{cyl}(r = D) = 2l_B\tau K_0[\kappa D]I_0[\kappa D]$, where K_0 and I_0 denote Bessel functions. Again, the limit of applicability of DH theory is defined by the condition $V_{cyl}(r = D) < 1$. For $\kappa D \ll 1$ the asymptotic behavior of the cylinder surface potential is given by (see Appendix A.2) $V_{cyl}(r = D) \simeq -2l_B\tau \ln(\kappa D)$ and the condition for DH to be valid becomes

$$1 > \kappa D > e^{-1/2\tau l_B} \tag{12}$$

This shows that for polymers below the Manning threshold, which means for weakly charged polymers with $\tau l_B < 1$, there is a wide range of salt concentrations for which the condition eq 12 can be fulfilled. For strongly charged polymers, with $\tau l_B > 1$, this range becomes very small for the case $\kappa D \ll 1$. On the other hand, in the limit $\kappa D > 1$ the asymptotic behavior of the cylinder surface potential is given by (see Appendix A.2) $V_{cyl}(r = D) \simeq l_B\tau/(\kappa D)$ and the condition for DH to be valid becomes

$$\kappa D > \tau l_B \tag{13}$$

This shows that in the high-salt case, $\kappa D > 1$, there is a wide range of salt concentrations where the Debye−Hückel approximation is valid even if the polymer is well above the Manning threshold. In all what follows, we restrict ourselves to the regime where the conditions eqs 11−13 are fulfilled.

C. Many-Chain Effects. In this section we generalize the discussion of the single-chain adsorption and consider the effect of interactions between different adsorbed polymers (or between different parts of one long adsorbed polymer, which is, for the present level of the discussion, the same). A strongly adsorbed, flat polymer phase can form a *disordered* surface pattern with many chain crossings, characterized by a certain mesh size B which corresponds to the average distance between chain crossings. We distinguish two different cases: if the effective persistence length l_{eff} is larger the mesh size, we obtain a disordered *uncrumpled* phase, as depicted schematically in Figure 2a; if the effective persistence length is smaller than the mesh size, we expect a phase which is *crumpled* between consecutive chain crossings, as depicted in Figure 2b. We also anticipate a *lamellar* phase where different polymer strands are parallel locally, characterized by an average lamellar spacing B, as shown in Figure 2c. The lamellar phase is stabilized either by steric or by electrostatic repulsions between neighboring polymers; we will in fact encounter both stabilization mechanisms for different values of the parameters.

We now calculate the free energy and other characteristics of these adsorbed phases. In all the following calculations, we assume that we are inside the adsorbed regime of a single polymer, as discussed in the previous section. In this case it is justified to neglect the repulsive free energy contribution due to the single-chain confinement, eq 3, and only consider the attractive component. We basically assume, later on, that the desorption

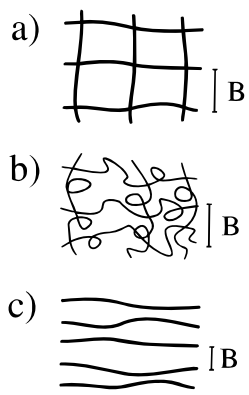

Figure 2. Schematic top views of the different adsorbed surface phases considered: (a) disordered uncrumpled phase, with an average mesh size B smaller than the persistence length, exhibiting an average density of chain crossings of $\sim 1/B^2$; (b) disordered crumpled phase, with a mesh size B larger than the persistence length; (c) lamellar phase, with a lamellar spacing B smaller than the persistence length.

transitions obtained for the single-chain case also describes many-chain adsorption.

Smeared-Out Limit. As we show in Appendix A.5, the electrostatic self-repulsion of an adsorbed polymer layer with a typical mesh size or lamellar spacing much smaller than the screening length exactly equals the self-energy of a smeared-out charge distribution. Strictly speaking, we demonstrate this in Appendix A.5 explicitly for a parallel and a square pattern, but we believe that the result remains true for *any* pattern, including disordered and crumpled ones. The smeared-out limit is therefore a universal limit which is obtained for any adsorbed phase when the typical length scale of the polymer structure becomes smaller than κ^{-1}.

The adsorption energy per unit area of a smeared-out charge distribution of thickness δ and surface charge density σ' follows from the electrostatic potential in eq A6 as

$$f_{att} = -\frac{4\pi l_B\sigma\sigma'}{\delta\kappa}\int_0^\delta e^{-\kappa z} = -\frac{4\pi l_B\sigma\sigma'(1 - e^{-\delta\kappa})}{\delta\kappa^2} \tag{14}$$

where σ denotes the substrate charge density. Minimizing the sum of the attraction to the substrate and the repulsion due to self-interaction within the adsorbed layer, eqs 14 and A24, the ratio of the adsorbed surface charge density and the substrate surface charge density follows as

$$\frac{\sigma'}{\sigma} = \frac{2\kappa\delta(1 - e^{-\delta\kappa})}{(e^{-2\delta\kappa} - 1 + 2\delta\kappa)} \tag{15}$$

which is graphically represented in Figure 3. In the limits of very small layer thickness, $\delta\kappa \to 0$, and very large layer thickness, $\delta\kappa \to \infty$, the adsorbed charge exactly compensates the substrate charge; i.e., we find $\sigma' \approx \sigma$. There is slight charge reversal for intermediate values of the layer thickness, with a maximal adsorbed charge of $\sigma' \approx 1.14\sigma$ for $\delta \approx 2.2\kappa^{-1}$. According to our scaling results for the polymer adsorption threshold, the equilibrium layer thickness is of the order of the screening length or smaller. This means that in the smeared-out limit, we predict a rather small over charging of about 10%. Clearly, the upper bound for the adsorbed amount is reached when the layer is close-packed, i.e., when $\sigma' \approx \tau/D$, which leads with the

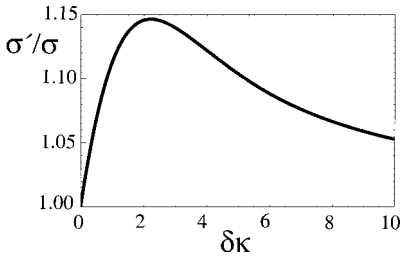

Figure 3. Ratio of the adsorbed surface charge density σ' and the substrate surface charge density σ as a function of the rescaled thickness δ of the adsorbed layer, obtained within a mean-field model where lateral charge correlations are neglected and the charge distribution is smeared out. There is a slight overcharging for layer thicknesses of the order of the screening length.

approximate relation $\sigma' \approx \sigma$ to an overfilling of the smeared-out phase for $\sigma > \sigma_{full}$ with

$$\sigma_{full} \sim \tau/D \tag{16}$$

Disordered (Uncrumpled) Case. We suppose now that the typical distance B between crossings is smaller than the effective persistence length (and that polymer strands are essentially straight between consecutive crossings as depicted in Figure 2a) but larger than the screening length, i.e. $\kappa^{-1} < B < l_{eff}$. In this case the main contribution to the electrostatic self-energy of the adsorbed layer comes from crossings and the repulsion between parallel strands can be neglected, as detailed in Appendix A.5.iii for the case of an ordered square pattern. The free energy density is given by

$$f_{dis} = 2W_{ads}/B + W_{cross}/B^2 \tag{17}$$

where the density of crossings is approximately B^{-2}, W_{ads} denotes the electrostatic adsorption energy per unit length (calculated in Appendix A.3), and W_{cross} denotes the electrostatic energy of a chain crossing (calculated in Appendix A.4). For $D\kappa < 1$ the free energy density is given by (using eqs A15 and A18)

$$f_{dis} = -4\pi l_B \kappa^{-1}\, \sigma\sigma' + \pi l_B \kappa^{-1} (\sigma')^2 \tag{18}$$

where we used the fact that the surface charge density of the adsorbed phase is $\sigma' \approx 2\tau/B$. Minimization leads to

$$\sigma' = 2\sigma \tag{19}$$

which means that the adsorbed charge overcompensates the substrate charge exactly by a factor of 2. This factor 2 of course may depend on our approximation of perpendicular crossings. We believe however that all our conclusions are not changed by a more accurate description of the crossings. The equilibrium mesh size follows as $B \approx \tau/\sigma$. The threshold for overfilling is $B \approx D$ and therefore is the same as given in eq 16 for the smeared-out case. Clearly, the free-energy expression eq 17 is only accurate and thus overcharging is expected only as long as the mesh size is larger than the screening length; if the mesh size becomes smaller than the screening length, a smeared-out adsorbed layer is obtained leading to exact charge compensation. The condition for charge reversal thus is $B \sim \tau/\sigma > \kappa^{-1}$, which can be reexpressed as $\sigma < \sigma_{rev}$ with

$$\sigma_{rev} \sim \tau\kappa \tag{20}$$

This has, up to numerical prefactors, the same scaling behavior as the image charge-induced desorption transition eq 9. For $\sigma > \sigma_{rev}$ one crosses over smoothly to the smeared-out case, where the adsorbed charge density exactly compensates the substrate charge. The equilibrium adsorption energy density equals the smeared-out adsorption energy and is given by $f_{dis} \sim f_{smear} \sim -l_B\kappa^{-1}\sigma^2$.

Lamellar Phase. We now consider the case where the adsorbed polymer forms a 2D lamellar phase; we assume that the distance between neighboring polymer strands, B, is much smaller than the effective persistence length, $B < l_{eff}$ (this assumption is checked self-consistently at the end). Since the possible conformations of the adsorbed polymers are severely restricted in the lateral directions, we have to include, in addition to the electrostatic interactions, a repulsive free energy contribution coming from steric interactions between stiff polymers.[30] The total free energy density is given by

$$f_{lam} \simeq \frac{W_{ads}}{B} + \frac{1}{l_{eff}^{1/3} B^{5/3}} \ln\left(\frac{l_{eff}}{B}\right) + f_{rep} \tag{21}$$

where the second term is the entropic Odijk repulsion and f_{rep} is the electrostatic repulsion of a lamellar array calculated in Appendix A.5.

For $D < \kappa^{-1} < B^* < B$ (with some crossover length B^*), the electrostatic repulsion between the polymers is irrelevant, and the effective free energy density can be written as (using eq A15)

$$f_{lam} \simeq -\frac{l_B\sigma\tau}{\kappa B} + \frac{1}{l_{eff}^{1/3} B^{5/3}} \ln\left(\frac{l_{eff}}{B}\right) \tag{22}$$

The lamellar phase is *sterically* stabilized in this case, and the preferred lamellar spacing is given by

$$B_{st} \sim \left[\frac{\kappa}{\tau\sigma l_B l_{eff}^{1/3}} \ln\left(\frac{\tau\sigma l_B l_{eff}}{\kappa}\right)\right]^{3/2} \tag{23}$$

In all what follows, we neglect the logarithmic cofactor. The free energy density in the equilibrium state is $f_{st} \sim -l_{eff}^{1/2}(\tau l_B\sigma/\kappa)^{5/2}$. Comparing this free energy with the free energy of the disordered phase, $f_{dis} \sim -l_B\kappa^{-1}\sigma^2$, the sterically stabilized lamellar phase is favored for $\sigma > \sigma_{st} \sim \kappa^3 l_B^{-3} l_{eff}^{-1}\tau^{-5}$. The adsorbed surface charge density in the sterically stabilized lamellar phase is $\sigma' \sim \tau/B_{st}$ and can, with the expression for B_{st}, eq 23, and the definition for σ_{st} be written as

$$\sigma' \simeq \sigma\left(\frac{\sigma}{\sigma_{st}}\right)^{1/2} \tag{24}$$

showing that the sterically stabilized lamellar phase is always overcharged when thermodynamically stable, i.e., when $\sigma > \sigma_{st}$.

For $D < \kappa^{-1} < B < B^*$, we expect the steric repulsion between the polymers to be irrelevant, and the effective free energy density is (using eqs A15 and A27)

$$f_{lam} \simeq -\frac{l_B\sigma\tau}{\kappa B} + \frac{l_B\tau^2 e^{-\kappa B}}{B^{3/2}\kappa^{1/2}} \tag{25}$$

This leads to the *electrostatically* stabilized lamellar spacing

$$B_{el} \sim \kappa^{-1} \ln\left[\frac{\tau\kappa}{\sigma}\right] \tag{26}$$

The adsorbed charge density then follows from $\sigma' \sim \tau/B_{el}$ as

$$\sigma' \sim \sigma \frac{\tau\kappa\sigma^{-1}}{\ln(\tau\kappa\sigma^{-1})} \tag{27}$$

Therefore, the electrostatically stabilized lamellar phase shows charge reversal as long as the spacing B is larger than the screening length. The free energy density scales as $f_{el} \sim -l_B\tau\sigma/\ln(\tau\kappa\sigma^{-1})$. The crossover between the sterically stabilized lamellar phase, described by eqs 22 and 23, and the lamellar phase which is stabilized by electrostatic repulsion, eqs 25 and 26, is determined by $B_{st} \sim B_{el} \equiv B^*$ leading to a crossover determined by (without logarithmic cofactors)

$$\sigma_{st/el} \sim \frac{\kappa^{5/3}}{\tau l_{eff}^{1/3} l_B} \tag{28}$$

This transition is exactly the same as the adsorption threshold in eq 5. It follows that the sterically stabilized lamellar phase only occurs in a logarithmically small window. For $\sigma > \sigma_{st/el}$, the distance between neighboring polymer strands is smaller than B^* and the electrostatic stabilization mechanism is at work; for $\sigma < \sigma_{st/el}$, the lamellar spacing B is larger than the characteristic crossover length B^* and the Odijk repulsion dominates. The electrostatically stabilized lamellar phase crosses over to the smeared-out (compensated) phase when B_{el} as given by eq 26 becomes of the order of the screening length κ^{-1}; this leads to the same transition threshold as the charge reversal transition, given in eq 20. The same transition threshold is found by comparing the free energy of the electrostatically stabilized lamellar phase with the disordered phase. This means that the disordered, the lamellar, and the smeared-out phases become simultaneously degenerate at the charge-reversal transition determined by eq 20. We thus expect the lamellar phase to be realized for $\sigma < \sigma_{rev}$ and the compensated phase to be stable for $\sigma > \sigma_{rev}$. On the other hand, we expect the sterically stabilized lamellar phase to crumple when B_{st} as given by eq 23 becomes larger than the effective persistence length l_{eff}. This threshold is not reached within the adsorbed phase; an adsorbed lamellar phase is therefore not crumpled.

In experiments on DNA adsorbed on oppositely charged substrates one typically observes a lamellar phase.[8,9] In one experiment, the spacing between DNA strands was found to increase with increasing salt concentration.[8] One theoretical explanation invokes an effective interaction between neighboring DNA strands mediated by elastic deformations of the membrane, which forms the substrate in these experiments.[35] In the sterically stabilized regime, the distance between adsorbed polymers increases as $B_{st} \sim \kappa^{3/2}$ with the salt concentration, see eq 23, which offers an alternative explanation for the experimental findings. It would be interesting to redo DNA adsorption experiments on rigid substrates, where the elastic coupling to the membrane is absent.

Crumpled Phase. The crumpled phase obtains if the mesh size B is both larger than the effective persistence length and the screening length, in which case the polymer crumples between consecutive crossings. Although the crumpled phase does not appear in our phase diagrams, we discuss briefly its characteristics. Denoting the contour length between two consecutive crossings as L, the mesh size is given by $B \sim l_{eff}^{1/4} L^{3/4}$, where we used the exact swelling exponent $\nu = 3/4$. The free energy density reads

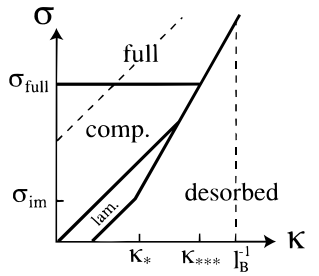

Figure 4. Complete adsorption phase diagram as a function of the substrate charge density σ and the inverse screening length κ. Note that we use logarithmic scales on both axes. We find a desorbed regime, an adsorbed lamellar phase (which is strongly overcharged), an adsorbed charge-compensated phase, and a full phase, where the substrate charge cannot be compensated with a single adsorption layer because the layer is close-packed. Our approximations to calculate the adsorption free energies are the Debye−Hückel approximation and the assumption that the polymers have vanishing thickness. These assumptions are only valid inside the region bounded by the broken lines.

$$f_{cr} = 2W_{ads}L/B^2 + W_{cross}/B^2 \tag{29}$$

For $D\kappa < 1$ the free energy density is

$$f_{cr} = -\frac{l_B\sigma\tau}{\kappa l_{eff}^{1/2} L^{1/2}} + \frac{l_B\tau^2}{\kappa l_{eff}^{1/2} L^{3/2}} \tag{30}$$

which upon minimization leads to $L \sim \tau/\sigma$ and thus $B_{cr} \sim l_{eff}^{1/4}(\tau/\sigma)^{3/4}$. The adsorbed surface charge density can be determined via $\sigma' \simeq \tau L/B_{cr}^2$ and is given by

$$\sigma' \simeq \sqrt{\frac{\tau\sigma}{l_{eff}}} \tag{31}$$

This can be rewritten as $\sigma' \simeq \sigma(L/l_{eff})^{1/2}$, which clearly demonstrates that the crumpled phase (which is defined by the fact that $L > l_{eff}$) is always overcharged. The free energy density is $f_{cr} \sim -l_B\kappa^{-1}\tau^{1/2}\sigma^{3/2}/l_{eff}^{1/2}$.

III. Phase Diagram

In Figure 4 we present the adsorption phase diagram for strongly charged polymers, defined by $\tau(l_B l_0)^{1/2} > 1$, as a function of the substrate charge density σ and the inverse screening length κ. We assumed in our discussion that the screening length is not too small; i.e., we restricted ourselves to the regime $\kappa l_B < 1$. This boundary is denoted by a broken line. For $\kappa l_B > 1$ the electrostatic interaction becomes effectively short ranged, and the present scaling description is not reliable. The region of validity of the DH approximation on the substrate surface is given by $\sigma < \kappa/l_B$ according to eq 11 and denoted by a broken line. We always assume that $l_0 > l_B$, a condition which is fulfilled in most practical cases, given that the bare persistence length of even the most flexible polymer comprises a couple of monomers due to fixed bond angles and hindered rotations. In the following we briefly discuss the most important scaling boundaries in the phase diagrams. We also assume the monomer radius D to be of the order of the Bjerrum

length l_B. This eliminates one further parameter, and it is a fairly accurate approximation for most polymers; it also means that we do not consider screening lengths smaller than the polymer diameter.

As discussed in details in Appendixes B and C, polyelectrolytes have for high values of their line charge density τ and screening length κ^{-1} an effective persistence length l_{eff} much higher than their bare persistence length l_0. In the last section we calculated free energies and phase boundaries as a function of the effective persistence length l_{eff}. Here we clarify to which extent this persistence length is modified by charge effects. Within our notation, it follows that for $\kappa < \kappa_{**} \equiv \tau l_B^{1/2}/l_0^{1/2}$ and $\tau(l_B l_0)^{1/2} > 1$ (the latter condition we always assume to be true in this paper) the effective persistence length l_{eff} is larger than the bare persistence length and given by $l_{OSF} = l_B\tau^2\kappa^{-2}/4$ (see Appendix B). For $\kappa > \kappa_{**}$, the effective persistence length equals the bare persistence length, i.e., $l_{eff} \approx l_0$.

The transitions from the lamellar phase to the desorbed phase are given in eqs 9 and 5. The crossover between the two transition lines occurs at $\kappa_* \sim \tau^3 l_B^{3/2} l_0^{1/2}$ and at a surface charge density σ_{im} given in eq 10. The lamellar phase is always electrostatically stabilized (up to a logarithmically narrow strip of the sterically stabilized phase close to the desorption transition) and shows strong charge reversal. The boundary to the compensated phase is given by eq 20. We predict a compensated phase which is not full for the parameter range $\sigma_{rev} < \sigma < \sigma_{full}$ as determined by eqs 16 and 20. We note that since the full phase is not charge reversed, the full phase exhibits a second adsorbed layer (or even more layers). It should however be clear that, at some point, the effective substrate charge density an additional layer feels is so small that the condition for adsorption is no longer met. The screening length where the electrostatic persistence length dominates over the bare persistence length is determined by $\kappa^{**} = \tau l_B^{1/2}/l_0^{1/2}$, and with our initial assumption that $\tau(l_B l_0)^{1/2} > 1$ we have $l_0^{-1} < \kappa_{**} < \kappa_*$, which means, at low enough salt concentrations such that the electrostatic chain stiffening becomes relevant, the desorption transition is induced by image-charge effects. The desorption transition meets the transition to a full adsorbed phase at $\kappa_{***} \equiv \tau^{6/5} l_0^{1/5}$, as follows by comparing eqs 9 and 16. There is a large region where the smeared-out calculation is valid, and the polymer forms a surface phase which is charge compensating and not close-packed. The location of the line $\kappa \sim l_B^{-1}$ with respect to the characteristic inverse screening lengths κ_* and κ_{***} depends on the value of the ratio l_0/l_B. For the phase diagram shown in Figure 4, we assumed $\kappa_* < \kappa_{***} < l_B^{-1}$; i.e., we assumed $(l_0/l_B)^{2/3} > \tau^2 l_B l_0$. This is the most general phase diagram, since it features both the desorption transition due to image-charge and entropic effects, for $\kappa < \kappa_*$ and $\kappa > \kappa_*$, respectively, from a phase which is not full. For many strongly charged and stiff polymers, as for example DNA, one in fact finds $l_B^{-1} < \kappa_{***} < \kappa_*$ and thus the desorption transition is always induced by image-charge effects. In this case the broken vertical line is moved to the left and the transition values κ_{***} and κ_* are outside the validity of our calculations.

The most important result is that there is a region where the substrate charge is strongly reversed and thus can give rise to multilayer formation if the adsorption of oppositely charged polymer is done in a second step. This charge reversal takes place in the form of a lamellar phase. The general trend that emerges is that charge reversal is more likely to occur for high salt concentrations and rather low substrate charge density. For too high salt concentration and too low substrate charge density, on the other hand, the polymer does not adsorb at all. In essence, the salt concentration and the substrate charge density have to be tuned to intermediate values in order to create charge multilayers.

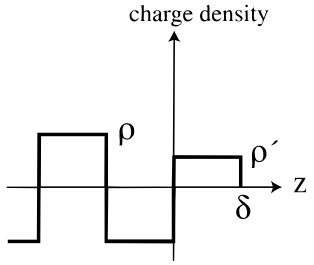

Figure 5. Schematic charge density distribution in a multilayer. We assume all layers to have the same thickness δ and the adsorbed sublayers to have charge densities of the same magnitude ρ. The charge density of the top layer is denoted as ρ'.

The adsorption diagram presented in Figure 4 has been obtained at a scaling level. In some cases the precise stability of the phases would require a precise calculation of the prefactors for the transition lines. We have made use of the calculated prefactors in our very rough approach. It should be noted, however, that, in some regions of the adsorption diagram, the phases are degenerate (at the scaling level) and that thermodynamically metastable phases could well be observed in practice.

IV. Scaling Limits for Multilayer Formation

In the preceding sections we have discussed the adsorption of semiflexible polymers on a homogeneously charged substrate. We have seen that there is a whole range of parameters for which the charge of the adsorbed polymer phase overcompensates the substrate charge. This charge reversal is interesting for several applications, as we briefly discuss in the summary. We saw that overcharging is always accompanied by a screening length κ^{-1} which is smaller than the typical mesh size B of the adsorbed layer (otherwise we can use the smearing-out approximation and always obtain, up to numerical factors of the order of unity, see eq 15, charge compensation). In this section we present some simple scaling results for the formation of multilayers. First, we show that multilayers do not form if the mesh size of the adsorbed polymer networks is smaller than the screening length. For this, we again use the smearing-out approximation. It thus follows that for the adsorption of a polymer layer on an oppositely charged adsorbed polymer layer (which plays the role of a substrate) the lower polymer layer cannot be regarded as homogeneously charged. Consequently, we present a simple scaling description of the adsorption of a polymer layer on an oppositely charged polymer layer, in section IV. B.

A. Smeared-Out Layer. The difference with the calculation for the adsorption of a smeared-out polymer distribution on a substrate is that now we can neglect substrate effects that are connected to image-charge effects and the impenetrability of the substrate for salt ions. The electrostatic interaction is therefore given by the bulk Debye−Hückel interaction, $v_{DH} = l_B e^{-\kappa r}/r$. In

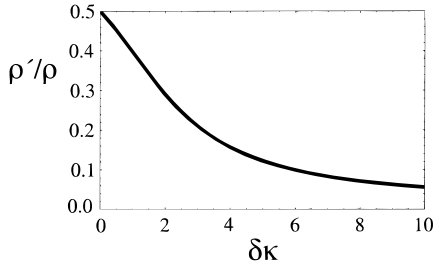

Figure 6. Result for the optimal rescaled charge density ρ'/ρ of the top layer of a smeared-out multilayer as a function of the rescaled layer thickness $\delta\kappa$. The charge density ratio is always smaller than $^1/_2$, which means that a smeared-out multilayer, which is a multilayer with a lateral meshsize smaller than the screening length, only supports a small number of layers.

the following we consider the adsorption of one polymer layer on an existing, charge-oscillating multilayer, which we assume to consist of individual polymer layers of thickness δ and volume-charge density ρ. We furthermore assume the top layer to have the same layer thickness δ and calculate the volume density of the top layer which we denote by ρ'. The charge density distribution is schematically plotted in Figure 5. The self-repulsive energy per unit area of the top layer is given by

$$f_{\mathrm{rep}} = \frac{2\pi(\rho')^2 l_{\mathrm{B}}}{\kappa} \int_0^\delta \mathrm{d}z \int_z^\delta \mathrm{d}z'\, \mathrm{e}^{-\kappa(z'-z)} \qquad (32)$$

which leads to the result

$$f_{\mathrm{rep}} = \frac{2\pi(\rho')^2 l_{\mathrm{B}}}{\kappa^3} (\mathrm{e}^{-\delta\kappa} - 1 + \delta\kappa) \qquad (33)$$

The interaction energy between the top layer and all adsorbed sublayers can be written as

$$f_{\mathrm{att}} = -\sum_{i=0}^{\infty} (-\mathrm{e}^{-\delta\kappa})^i \frac{2\pi\rho\rho' l_{\mathrm{B}}}{\kappa} \int_0^\delta \mathrm{d}z \int_0^\delta \mathrm{d}z'\, \mathrm{e}^{-\kappa(z'+z)} \qquad (34)$$

where the sum takes into account the interaction of the top layer with all layers underneath. One notes that the oscillating charge distribution requires a minus sign in the parentheses, giving an attractive interaction with the nearest-neighbor layer, a repulsive interaction with the second-nearest-neighbor layer, and so on. Using that $\sum_{i=0}^{\infty} (-p)^i = 1/(1+p)$, the total interaction is

$$f_{\mathrm{att}} = -\frac{2\pi\rho\rho' l_{\mathrm{B}}}{\kappa^3} (1 - \mathrm{e}^{-\delta\kappa})^2 (1 + \mathrm{e}^{-\delta\kappa})^{-1} \qquad (35)$$

The charge density of the top layer, ρ', follows by taking a derivative of the total free energy density $f = f_{\mathrm{att}} + f_{\mathrm{rep}}$ with respect to ρ' and reads

$$\frac{\rho'}{\rho} = \frac{(1 - \mathrm{e}^{-\delta\kappa})^2}{2(1 + \mathrm{e}^{-\delta\kappa})(\mathrm{e}^{-\delta\kappa} - 1 + \delta\kappa)} \qquad (36)$$

In Figure 6 we plot the charge density ratio ρ'/ρ as a function of the rescaled layer thickness $\delta\kappa$. This ratio approaches a value of one-half, as the layer thickness becomes much smaller than the screening length, and monotonically decreases to zero as the thickness increases. We therefore obtain the important result that a smeared-out multilayer does not lead to the adsorption of a top layer with the same charge density as the layers underneath and thus does not lead to the propagation of charge oscillation. This result is related to the fact that we assume that salt ions penetrate into the multilayer, which effectively screens all electrostatic interactions. But we note that even if we do not allow salt ions to enter the multilayer (which corresponds to $\kappa = 0$), we obtain the asymptotic ratio of $\rho'/\rho = {}^1/_2$, which is still not sufficient to generate a multilayer structure. We thus have to consider the possibility of a multilayer with a lateral structure with a mesh size larger than the screening length, as done in the following section.

A second way to generate a larger charge of the top layer would be to induce some vertical charge separation in each layer, for example by having a bimodal vertical charge distribution in each layer which is peaked at the top and the bottom. Experimentally, this could be achieved by using polymers which have charged groups which are not distributed evenly around the polymer but which point in two opposite directions. If the polymers orient with the charged groups pointing normal to the substrate, a stronger overcharging should result. Such detailed architectural questions we will not consider further in this paper. A third way to stabilize multilayers involves short-ranged, non-electrostatic attractions between polymers. This point is particularly important for polyelectrolytes with hydrophobic backbones, as will be detailed in subsequent publications.

B. Discrete Case. As for the case of a homogeneously charged substrate, we distinguish between a disordered (uncrumpled) phase as depicted in Figure 2a with a mesh size B, where the average surface charge density is given by $\sigma' \simeq 2\tau/B_{\mathrm{dis}}$, and a disordered crumpled phase as depicted in Figure 2b, where the average surface charge density is $\sigma' \simeq 2L\tau/B_{\mathrm{cr}}{}^2 \simeq 2\tau/B_{\mathrm{cr}}{}^{2/3} l_{\mathrm{eff}}{}^{1/3}$ where we have used $B_{\mathrm{cr}} \simeq l_{\mathrm{eff}}{}^{1/4} L^{3/4}$. We do not explicitly consider the case of a lamellar adsorbed phase (our results in the previous sections show that, on a scaling level, there is no difference between a lamellar and a charge-reversing disordered phase, and more importantly, a lamellar structure leads to complicated effects which have to do with the coupling between consecutive layers). In the limit that the mesh size is larger than the screening length, the repulsive self-energy of an adsorbing layer is dominated by crossings and thus given by $f_{\mathrm{rep}} \simeq W_{\mathrm{cross}}/B^2$ leading to

$$f_{\mathrm{rep}} \simeq W_{\mathrm{cross}} \frac{(\sigma')^2}{4\tau^2} \qquad (37)$$

for the disordered (uncrumpled) phase and

$$f_{\mathrm{rep}} \simeq W_{\mathrm{cross}} \frac{(\sigma')^3 l_{\mathrm{eff}}}{8\tau^3} \qquad (38)$$

for the crumpled phase. The attractive energy between the substrate layer and the adsorbing layer is

$$f_{\mathrm{att}} \simeq W_{\mathrm{cross}} \frac{\sigma\sigma'}{2\tau^2} \qquad (39)$$

regardless of whether the adsorbing phase is crumpled or not, where σ is the average surface charge density of the lower polymer layer. Minimizing the effective free energy density $f = f_{\mathrm{rep}} + f_{\mathrm{att}}$ with respect to the charge

density of the adsorbing polymer layer, σ', we obtain

$$\sigma' = \sigma \tag{40}$$

for the uncrumpled phase and

$$\sigma' = \sigma \sqrt{\frac{4\tau}{3l_{\text{eff}}\sigma}} \tag{41}$$

for the crumpled phase. For the uncrumpled phase, we see that the adsorbed layer has the same surface charge density as the substrate layer. Assuming that the screening length is of the order of the distance between consecutive adsorbing layers, such that repulsive interactions between next-nearest-neighbor layers are unimportant, multilayers can form. Interestingly, we see that the specific form of W_{cross}, which depends on the monomer size, line charge density, and so on, does not enter into the results for the adsorbate charge density. The crumpled phase is only realized for $B > l_{\text{eff}}$, which is using eq 41 equivalent to $\tau/l_{\text{eff}}\sigma > 1$. This means that, since the factor in the square root in eq 41 is larger than unity, the charge of the adsorbed layer is larger than the one of the lower layer. Multiplying both sides of eq 41 by $3l_{\text{eff}}/4\tau$, one obtains the equation

$$\frac{3l_{\text{eff}}\sigma'}{4\tau} = \sqrt{\frac{3l_{\text{eff}}\sigma}{4\tau}} \tag{42}$$

which can be interpreted as a nonlinear map relating the lower layer charge density with the (upper) adsorbing layer charge density. If one assumes that a large number of layers adsorb, one can easily see that the charge of each adsorbed layer increases until the threshold between the crumpled and uncrumpled phase is reached, i.e., until

$$\frac{3l_{\text{eff}}\sigma'}{4\tau} = \frac{3l_{\text{eff}}\sigma}{4\tau} = 1 \tag{43}$$

and thus $B \simeq l_{\text{eff}}$ is reached, which is a *fixed point* of this nonlinear map. It thus seems that, once one allows for a sufficiently coarse adsorbed layer structure with a mesh size larger than the screening length, the formation of charge oscillating multilayer is unavoidable. Of course, one has to keep in mind that still the conditions for the formation of an adsorbed layer, which have been presented in the preceding sections, have to be satisfied.

V. Summary

In this article we treat the adsorption of strongly charged semiflexible polymers with $\tau(l_B l_0)^{1/2} > 1$ on flat, oppositely charged substrates. Multichain effects are taken into account on a simplified scaling level. We explicitly include lateral correlation effects by considering different lateral layer organizations. All electrostatic interactions are treated within the Debye−Hückel approximation, which limits the applicability of our results to a rather narrow window in the parameter space. On the other hand, the restriction to DH allows us to treat all electrostatic interactions consistently on the same level. We obtain adsorbed phases which are confined over a vertical thickness less than the screening length. As adsorbed phases, we obtain a lamellar phase, which can be stabilized by either electrostatic or steric lateral repulsions, and a disordered phase. If the average mesh size or lamellar spacing of the adsorbed phase is smaller than the screening length, we obtain charge compensation; i.e., the charge of the adsorbed phase exactly compensates the substrate charge (up to numerical factors of the order of unity). If, on the other hand, the typical mesh size is larger than the screening length, strong charge reversal occurs. This charge reversal for example allows, in a subsequent adsorption process of oppositely charged polyelectrolytes, for the formation of multilayers. Charge reversal is also a driving force for the controlled flocculation of colloidal dispersions, since a second colloidal particles which carries no adsorbed polymer would electrostatically bind to the overcharged region. It is clear that flocculation occurs when the overall concentration of polymer in the solution is low such that only part of the colloidal surface area is covered with polymers. On the other hand, in the case of excess polymer, the total charge of colloidal particles can be reversed and thus lead to enhanced stabilization of colloidal dispersions. As our main result, we present the complete adsorption phase diagram as a function of the inverse screening length and the surface charge density; see Figure 4.

The charge reversal mechanism discussed here is complementary to the charge reversal seen in mean-field and self-consistent type calculations:[25−27] There charge reversal is due to the fact that the adsorbed layer extends into the vertical direction over a distance comparable to or larger than the screening length, in which case the charge reversal is caused by dangling loops and tails. In the present case of strong adsorption, i.e., where one has a practically two-dimensional monomolecular layer of adsorbed polymers, it is important to not use a mean-field description of the layer, treating the charge as smeared-out, but to treat lateral correlations between the adsorbed polymer strands. We neglected nonelectrostatic interactions between the polymers and the substrate. If these interactions are attractive, they can lead to overcharging of the substrate even if the adsorbed layer can be treated as a smeared-out charge distribution. The description adopted here seems best to fit experiments on adsorption of DNA on membranes and flat substrates,[8−10] but flat adsorbed layers have also been reported for strongly charged synthetic polyelectrolytes.[7,11,12]

Appendix A: Electrostatic Interactions

In the presence of a solution of mobile salt ions, electrostatic interactions are exponentially screened for large separations. Two point charges interact via the Debye−Hückel potential

$$v_{\text{DH}}(r) = \frac{l_B e^{-\kappa r}}{r} \tag{A1}$$

where the screening length κ^{-1} is defined via $\kappa^2 = 4\pi l_B I$ and the ionic strength of a symmetric ionic solution of valency z and concentration c is $I = 2z^2c$. In the vicinity of a solid substrate, the simple Debye−Hückel potential in eq A1 is modified due to dielectric boundary effects and because salt ions cannot penetrate into the substrate. For a substrate of dielectric constant ϵ' the electrostatic interaction between two unit charges is defined via the 2D Fourier transformation

$$\tilde{v}_{\text{DH}}(\mathbf{r}, \mathbf{r}') = \int_0^\infty \frac{dp}{2\pi}\, p J_0[p r_{||}] \tilde{v}_{\text{DH}}(z, z', p) \tag{A2}$$

where J_0 is the zeroth-order Bessel function and the Green's function reads[36]

$$\tilde{\nu}_{\mathrm{DH}}(z, z', p) = \frac{2\pi l_{\mathrm{B}}}{\sqrt{\kappa^2 + p^2}}\left[\mathrm{e}^{-|z-z'|\sqrt{\kappa^2+p^2}} + \frac{\sqrt{\kappa^2+p^2} - \epsilon' p/\epsilon}{\sqrt{\kappa^2+p^2} + \epsilon' p/\epsilon}\mathrm{e}^{-(z+z')\sqrt{\kappa^2+p^2}}\right] \quad \text{(A3)}$$

In general, the DH interaction in the presence of a wall is quite complicated and the integral in eq A2 can only be calculated explicitly for certain limits. For solids with a dielectric constant much smaller than the dielectric constant of water, it is permitted to approximately set $\epsilon'/\epsilon \approx 0$, in which case the DH interaction at an impenetrable wall becomes

$$\tilde{\nu}_{\mathrm{DH}}(\mathbf{r}, \mathbf{r}') = \frac{l_{\mathrm{B}}\mathrm{e}^{-\kappa|\mathbf{r}-\mathbf{r}'|}}{|\mathbf{r} - \mathbf{r}'|} + \frac{l_{\mathrm{B}}\mathrm{e}^{-\kappa\sqrt{(\mathbf{r}-\mathbf{r}')^2+4zz'}}}{\sqrt{(\mathbf{r} - \mathbf{r}')^2 + 4zz'}} \quad \text{(A4)}$$

The potential at contact, i.e. $z = z' = 0$, is twice the ordinary DH potential in eq A1, and for large separations from the substrate the interaction smoothly goes over to the ordinary DH potential. In most cases and relatively close to the wall, it is therefore sufficient to consider the effect of a low-dielectric wall by an enhancement factor of 2 over the ordinary DH potential, i.e., to assume that $\tilde{\nu}_{\mathrm{DH}}(\mathbf{r}, \mathbf{r}') \approx 2\nu_{\mathrm{DH}}(|\mathbf{r} - \mathbf{r}'|)$. For a metal, on the other hand, the dielectric constant is practically infinity, and the interaction between two charges is

$$\tilde{\nu}_{\mathrm{DH}}(\mathbf{r}, \mathbf{r}') = \frac{l_{\mathrm{B}}\mathrm{e}^{-\kappa|\mathbf{r}-\mathbf{r}'|}}{|\mathbf{r} - \mathbf{r}'|} - \frac{l_{\mathrm{B}}\mathrm{e}^{-\kappa\sqrt{(\mathbf{r}-\mathbf{r}')^2+4zz'}}}{\sqrt{(\mathbf{r} - \mathbf{r}')^2 + 4zz'}} \quad \text{(A5)}$$

Close to the wall, the two terms in eq A5 cancel and electrostatic interactions become very small.

The potential created by a constant surface charge density σ, which follows from eq A3 as $V_{\mathrm{plane}}(z) = \sigma\tilde{\nu}_{\mathrm{DH}}(z, z' = 0, p = 0)$, reads

$$V_{\mathrm{plane}}(z) = 4\pi l_{\mathrm{B}}\sigma\kappa^{-1}\,\mathrm{e}^{-\kappa z} \quad \text{(A6)}$$

and is independent of the substrate dielectric constant. Note that the total interaction of a charge with a substrate always contains additional self-energy contributions, which are calculated in the next section.

1. Self-Energy of a Charged Polymer at a Substrate. The self-energy of a charged polymer in the vicinity of a solid substrate contains a repulsive contribution, due to the decrease in screening because there are no ions inside the substrate, and a contribution, due to dielectric boundary effects, which can be attractive or repulsive. Per unit length of the polymer, this self-energy is as a function of the distance from the substrate given by[36]

$$f_{\mathrm{self}}(z) = \frac{\tau^2}{2}\int_{-\infty}^{\infty}\mathrm{d}s\int_{-\infty}^{\infty}\frac{\mathrm{d}p_x}{2\pi}\int_{-\infty}^{\infty}\frac{\mathrm{d}p_y}{2\pi}\times \mathrm{e}^{ip_y s}\,\tilde{\nu}_{\mathrm{DH}}(z, z, \sqrt{{p_x}^2 + {p_y}^2}) \quad \text{(A7)}$$

Using Green's function eq A3 and subtracting off the self-energy infinitely far away from the substrate, we obtain for the self-energy difference

$$\Delta f_{\mathrm{self}} = l_{\mathrm{B}}\tau^2\int_0^{\infty}\frac{\mathrm{d}p}{\sqrt{\kappa^2 + p^2}}\frac{\sqrt{\kappa^2 + p^2} - \epsilon' p/\epsilon}{\sqrt{\kappa^2 + p^2} + \epsilon' p/\epsilon}\,\mathrm{e}^{-2z\sqrt{\kappa^2+p^2}} \quad \text{(A8)}$$

In the limit $\epsilon'/\epsilon = 0$, which corresponds to a substrate with a very small dielectric constant, the integral gives

$$\Delta f_{\mathrm{self}}(z) = l_{\mathrm{B}}\tau^2 K_0[2\kappa z] \quad \text{(A9)}$$

For small arguments the Bessel function goes like $K_0[x] \sim -\ln(x)$. If one neglects the logarithmic factor, the repulsion is of the order of $l_{\mathrm{B}}\tau^2$. In the limit $\epsilon'/\epsilon = \infty$, corresponding to adsorption on a metal substrate, we obtain the same result as in eq A9 but with a negative sign. In this case, there is an overall attraction to the substrate (even if the substrate is not charged). If the dielectric constants of the fluid and the substrate are the same, we obtain

$$\Delta f_{\mathrm{self}}(z) = \frac{l_{\mathrm{B}}\tau^2}{2}\left(K_0[2\kappa z] + K_2[2\kappa z] - \frac{1 + 2\kappa z}{z^2\kappa^2}\,\mathrm{e}^{-2\kappa z} + \frac{K_1[2\kappa z]}{z\kappa}\right) \quad \text{(A10)}$$

For small separation, we obtain from eq A10 the asymptotic expansion $\Delta f_{\mathrm{self}}(z) \simeq l_{\mathrm{B}}\tau^2(1/2 - 4z\kappa/3)$, and for large separations, the result is $\Delta f_{\mathrm{self}}(z) \simeq l_{\mathrm{B}}\tau^2\mathrm{e}^{-2z\kappa}\sqrt{\pi/4z\kappa}$. There is therefore a strong repulsion from the wall, which is for small separations of the order of $l_{\mathrm{B}}\tau^2$ per polymer unit length and which is due to the fact that there are no mobile ions inside the substrate. This repulsion is therefore solely due to the absence of screening in one-half space.

2. Surface Potential of a Charged Cylinder. The reduced potential created by a charged line with line charge density τ at a distance r is within the Debye–Hückel approximation given by

$$V_{\mathrm{line}}(r) = \tau\int_{-\infty}^{\infty}\mathrm{d}s\;\nu_{\mathrm{DH}}(\sqrt{r^2 + s^2}) = 2l_{\mathrm{B}}\tau K_0[\kappa r] \quad \text{(A11)}$$

With this result, the surface potential of a cylinder of finite radius D and surface charge density $\tau/(2\pi D)$ (and neglecting image charge effects and the impenetrability of the cylinder for salt ions) follows as

$$V_{\mathrm{cyl}}(r = D) = 2l_{\mathrm{B}}\tau\int_0^{2\pi}\frac{\mathrm{d}\phi}{2\pi}K_0[2\kappa D\,\sin(\phi/2)] = 2l_{\mathrm{B}}\tau K_0[\kappa D]I_0[\kappa D] \quad \text{(A12)}$$

Using the asymptotic expansions of the modified Bessel functions K_0 and I_0, the limiting forms of the surface potential are $V_{\mathrm{cyl}}(D) \simeq l_{\mathrm{B}}\tau/(\kappa D)$ and $V_{\mathrm{cyl}}(D) \simeq -2l_{\mathrm{B}}\tau\ln(\kappa D)$ for $\kappa D \gg 1$ and $\kappa D \ll 1$, respectively.

3. Adsorption Energy of a Cylinder on a Charged Plane. Using the reduced electrostatic potential created by a homogeneously charged plane with surface charge density σ, eq A6, the attraction between a charged rod of radius D and surface charge density $\tau/(2\pi D)$ and a charged wall is per unit length given by

$$W_{\mathrm{ads}}(z) = -\tau\int_0^{2\pi}\frac{\mathrm{d}\phi}{2\pi}\,V_{\mathrm{plane}}(z + \mathrm{D}\cos\phi) \quad \text{(A13)}$$

where z is the distance between the cylinder center and the surface. The integral gives

$$W_{ads}(z) = -4\pi l_B \kappa^{-1}\, \sigma\tau I_0[\kappa D] e^{-\kappa z} \qquad \text{(A14)}$$

The limiting results for the attraction at contact, i.e. for $W_{ads}(z = D)$, are

$$W_{ads} \simeq \begin{cases} -4\pi l_B \kappa^{-1} \sigma\tau & \text{for } \kappa D \ll 1 \\ -\sqrt{8\pi} l_B \kappa^{-3/2} \sigma\tau D^{-1/2} & \text{for } \kappa D \gg 1 \end{cases} \qquad \text{(A15)}$$

4. Two Crossing Cylinders. The repulsion between two perpendicular charged lines with a closest distance of r is

$$W_{cross}(r) = l_B \tau^2 \int_{-\infty}^{\infty} ds_1\, ds_2\, \frac{e^{-\kappa\sqrt{s_1^2+s_2^2+r^2}}}{\sqrt{s_1^2 + s_2^2 + r^2}} \qquad \text{(A16)}$$

leading to the closed-form result[37]

$$W_{cross}(r) = 2\pi l_B \tau^2\, \kappa^{-1}\, e^{-\kappa r} \qquad \text{(A17)}$$

In the limit $r \to 0$, that is when the cylinders touch, this leads to

$$W_{cross} = 2\pi l_B \tau^2 \kappa^{-1} = 8\pi l_{OSF} \kappa \qquad \text{(A18)}$$

where we used the definition eq C3 for the electrostatic persistence length $l_{OSF} = l_B\tau^2/4\kappa^2$. If the two crossing cylinders are close (within a screening length) to a low-dielectric substrate, the crossing energy is enhanced by a factor of approximately 2 (compare the discussion in the beginning of this section). If, on the other hand, the crossing cylinders are close to a metal, the crossing energy is exponentially small. The crossing energy of two touching cylinders of finite radius D with the charges smeared out over the cylinder surfaces is

$$W_{cross} = l_B \tau^2 \int_{-\infty}^{\infty} ds_1\, ds_2 \int_0^{2\pi} \frac{d\phi_1\, d\phi_2}{4\pi^2} \times \frac{e^{-\kappa\sqrt{s_1^2+s_2^2+D^2(2+\cos\phi_1+\cos\phi_2)^2}}}{\sqrt{s_1^2 + s_2^2 + D^2(2 + \cos\phi_1 + \cos\phi_2)^2}} \qquad \text{(A19)}$$

Using the result eq A17 we obtain

$$W_{cross} = \frac{l_B \tau^2}{2\pi\kappa} \int_0^{2\pi} d\phi_1\, d\phi_2\, e^{-\kappa D(2+\cos\phi_1+\cos\phi_2)} \qquad \text{(A20)}$$

In the limit $\kappa D \ll 1$ we are led back to eq A18. In the opposite limit, $\kappa D \gg 1$, we obtain with a straightforward saddle-point analysis

$$W_{cross} \sim \frac{l_B \tau^2}{\kappa^2 D} \sim \frac{l_{OSF}}{D} \qquad \text{(A21)}$$

In an adsorbed layer with many chain crossings, the structure is disordered and the crossings are not exactly perpendicular. For a finite crossing angle, the crossing energy has a similar scaling behavior but with an angular factor. The averaging over the crossing angle may then only change the prefactor in eq A18.

5. Electrostatic Self-Energy of Adsorbed Polymer Layers. *i. The Smeared-Out Case.* The repulsive free energy per unit area of a smeared-out charge distribution of surface charge density σ' and thickness δ is

$$f_{rep} = \frac{(\sigma')^2}{2\delta^2} \int_0^{\delta} dz\, dz'\, \tilde{v}_{DH}(z, z', p = 0) \qquad \text{(A22)}$$

From eq A3 we obtain straightforwardly

$$\tilde{v}_{DH}(z, z', p = 0) = \frac{2\pi l_B}{\kappa} (e^{-|z-z'|\kappa} + e^{-(z-z')\kappa}) \qquad \text{(A23)}$$

and thus from eq A22 the final result

$$f_{rep} = \frac{\pi l_B (\sigma')^2}{\delta^2 \kappa^3} (e^{-2\delta\kappa} - 1 + 2\delta\kappa) \qquad \text{(A24)}$$

with the limits $f_{rep} \sim 2\pi l_B(\sigma')^2\kappa^{-1}$ for $\delta \ll \kappa^{-1}$ and $f_{rep} \sim 2\pi l_B(\sigma')^2\, \delta^{-1}\kappa^{-2}$ for $\delta \gg \kappa^{-1}$.

ii. Parallel Polymers. The repulsive electrostatic free energy density of an array of parallel lines with a nearest-neighbor distance of B and line charge density τ can with the result for the potential of a charged line, eq A11, be written as

$$f_{rep} = \frac{2 l_B \tau^2}{B} \sum_{j=1}^{\infty} K_0[jB\kappa)] \qquad \text{(A25)}$$

This expression is also accurate for rods of finite radius D as long as $D \ll B$ holds. In the limit $B\kappa \ll 1$, when the distance between strands is much smaller than the screening length, the sum can be transformed into an integral and we obtain

$$f_{rep} \simeq \frac{2 l_B \tau^2}{B} \int_0^{\infty} ds\, K_0[sB\kappa)] = \frac{\pi l_B \tau^2}{B^2 \kappa} \qquad \text{(A26)}$$

This expression neglects effects due to the presence of a solid substrate. As discussed above, for a low-dielectric substrate the electrostatic interactions are enhanced by a factor of 2 close to the substrate surface. Since the average surface charge density is given by $\sigma' = \tau/B$, it follows that the self-energy eq A26 in the limit $B\kappa \ll 1$ is given by $f_{rep} \simeq \pi l_B(\sigma')^2\kappa^{-1}$ and thus identical to the asymptotic result for the smeared-out case, eq A24, if one corrects by the factor of 2 for the substrate influence on the electrostatic interaction.

In the opposite limit, $B\kappa \gg 1$, when the polymers are much farther apart than the screening length, the sum in eq A25 is dominated by the first term, and with asymptotic expansion of the Bessel function the free energy density becomes

$$f_{rep} \simeq \frac{\sqrt{2\pi} l_B \tau^2 e^{-B\kappa}}{B^{3/2}\kappa^{1/2}} \qquad \text{(A27)}$$

In this limit, it is important to note that the smeared-out repulsive energy eq A24 is much larger and thus considerably overestimates the actual electrostatic repulsion between polymer strands.

iii. Square Pattern. In this case we assume the polymers to form a perfectly ordered square lattice with nearest-neighbor distance B. It is easy to see that the repulsive energy can be separated into a part coming from interactions between parallel polymers and a part coming from perpendicular polymers, i.e., coming from crossings. Since there is one crossing per area B^2, the

total repulsive free energy is exactly

$$f_{\mathrm{rep}} = \frac{4l_{\mathrm{B}}\tau^2}{B}\sum_{j=1}^{\infty} K_0[jB\kappa)] + \frac{W_{\mathrm{cross}}}{B^2} \qquad \text{(A28)}$$

where the free energy of one crossing is given in eqs A18 and A21. In the limit $B\kappa \ll 1$ (and, since $D < B$, also $D\kappa \ll 1$) we obtain, using the same calculation leading to eq A26, the simple result

$$f_{\mathrm{rep}} \simeq \frac{4\pi l_{\mathrm{B}}\tau^2}{B^2\kappa} \simeq \frac{\pi l_{\mathrm{B}}(\sigma')^2}{\kappa} \qquad \text{(A29)}$$

which is identical to the smeared-out result, eq A24, if we account for the dielectric jump at the substrate surface by an enhancement factor of 2. Here we used that for the square pattern the average charge density is $\sigma' = 2\tau/B$. In the limit $B\kappa \gg 1$ the contribution coming from the repulsion between parallel strands is negligible. For $D\kappa < 1$ we obtain

$$f_{\mathrm{rep}} \simeq \frac{2\pi l_{\mathrm{B}}\tau^2}{B^2\kappa} \simeq \frac{\pi l_{\mathrm{B}}(\sigma')^2}{2\kappa} \qquad \text{(A30)}$$

which exactly equals half the previous result, eq 29. For $D\kappa > 1$ the resultant repulsive energy is

$$f_{\mathrm{rep}} \sim \frac{l_{\mathrm{B}}\tau^2}{B^2\kappa D} \sim \frac{l_{\mathrm{B}}(\sigma')^2}{\kappa D} \qquad \text{(A31)}$$

Appendix B: Electrostatic Persistence Length at a Substrate

Here we calculate the chain stiffening due to the electrostatic repulsion between monomers for a polymer that is adsorbed on a substrate. To simplify the calculation, we assume the polymer to lie flat on the substrate surface. If the dielectric constant ratio ϵ'/ϵ is treated as an expansion parameter, the electrostatic interaction between two charges at the surface follows from eqs A2 and A3 as

$$\tilde{v}_{\mathrm{DH}}(r_{\|}) \simeq \frac{2l_{\mathrm{B}}\mathrm{e}^{-\kappa r_{\|}}}{r_{\|}} + \frac{2\epsilon' l_{\mathrm{B}}}{\epsilon r_{\|}} \times \begin{cases} -1 & \text{for } r_{\|} \ll \kappa^{-1} \\ r_{\|}^{-2}\kappa^{-2} & \text{for } r_{\|} \gg \kappa^{-1} \end{cases} \qquad \text{(B1)}$$

In the limit $\epsilon'/\epsilon = 0$ the electrostatic interaction is simply enhanced by a factor of 2. It follows that the electrostatic persistence length in this limit is twice as large as in the bulk case. For finite values of ϵ'/ϵ the interaction at large distances decays algebraically as an inverse cube of the distance.[38] This behavior can be easily understood because each charge forms at the substrate interface a dipole consisting of the charge and, at a distance of the order of the screening length, the neutralizing counterion cloud. Since the dipole−dipole interaction which is mediated by the substrate half-space is not screened, we obtain the inverse cubic interaction. The effective electrostatic persistence length can be calculated from the electrostatic self-energy of a circle of bending radius R. Since the total bending energy of such a circle is $l_{\mathrm{eff}}\pi/R$, the persistence length follows as

$$l_{\mathrm{eff}} = \frac{\tau^2 R^3}{\pi}\int_0^{2\pi}\mathrm{d}\gamma \int_{\gamma}^{2\pi}\mathrm{d}\gamma' \times \left\{\tilde{v}_{\mathrm{DH}}\left(2R\sin\left[\frac{\gamma'-\gamma}{2}\right]\right) - \tilde{v}_{\mathrm{DH}}(R[\gamma'-\gamma])\right\} \qquad \text{(B2)}$$

where we subtract the self-energy of a straight polymer segment of the same length. Since the inverse cubic interaction leads to a logarithmic divergence for large distances, we use as an effective cutoff the persistence length and obtain as the electrostatic persistence length the result

$$l_{\mathrm{eff}} \simeq 2l_{\mathrm{OSF}}\left(1 - \frac{\epsilon'}{6\epsilon} + \frac{\epsilon'}{\epsilon}\ln[2l_{\mathrm{OSF}}\kappa]\right) \qquad \text{(B3)}$$

where the persistence length in the bulk is given by $l_{\mathrm{OSF}} = l_{\mathrm{B}}\tau^2/4\kappa^2$. As one can see, there is a logarithmic correction to the persistence length, which however, for most practical cases, since ϵ'/ϵ is typically quite small, can be neglected.

Appendix C: Scaling Behavior of a Single Semiflexible Polyelectrolyte Chain

Here we derive the complete scaling behavior of the effective persistence length of a single semiflexible PE. This calculation is a trivial extension of the results for a flexible PE, so we can be brief. The electrostatic energy of a sphere of charge Q and radius R is $W_{\mathrm{el}}/k_{\mathrm{B}}T \simeq l_{\mathrm{B}}Q^2/R$. The exact charge distribution (e.g., constant volume charge density versus charge distributed on the surface only) only changes the prefactor of order unity and is therefore unimportant. For a polymer of length L and line charge density τ the total charge is $Q = \tau L$. The polymer radius depends in addition on the bare persistence length l_0 and reads $R = (l_0 L)^{1/2}$. We thus obtain for the electrostatic energy of a (roughly spherical) polymer coil $W_{\mathrm{el}}/k_{\mathrm{B}}T \simeq l_{\mathrm{B}}\tau^2 L^{3/2} l_0^{-1/2}$. The polymer length at which the electrostatic self-energy is of order $k_{\mathrm{B}}T$, i.e., $W_{\mathrm{el}}/k_{\mathrm{B}}T \simeq 1$, follows as

$$L_{\mathrm{el}} \simeq l_0(l_{\mathrm{B}}l_0\tau^2)^{-2/3} \qquad \text{(C1)}$$

and defines the electrostatic blob size or electrostatic polymer length. We expect a locally crumpled polymer configuration if $L_{\mathrm{el}} > l_0$; i.e., if $l_{\mathrm{B}}\tau < (l_{\mathrm{B}}/l_0)^{1/2}$. Conversely, for $l_{\mathrm{B}}\tau > (l_{\mathrm{B}}/l_0)^{1/2}$, the polymer remains locally stiff even for contour lengths larger than the bare persistence length l_0 and the effective persistence length is given by

$$l_{\mathrm{eff}} \simeq l_0 + l_{\mathrm{OSF}} \qquad \text{(C2)}$$

where the electrostatic persistence length, first calculated by Odijk, Skolnick, and Fixman, is given by

$$l_{\mathrm{OSF}} = \frac{l_{\mathrm{B}}\tau^2}{4\kappa^2} \qquad \text{(C3)}$$

The electrostatic persistence length of course only gives a sizable contribution to the effective persistence length for $l_{\mathrm{OSF}} > l_0$, which is equivalent to $l_{\mathrm{B}}\tau > (l_{\mathrm{B}}l_0)^{1/2}\kappa$. For the case where the polymer crumples on length scales larger than the bare bending rigidity, i.e., for $L_{\mathrm{el}} > l_0$ or $l_{\mathrm{B}}\tau < (l_{\mathrm{B}}/l_0)^{1/2}$, the perturbative approach used for the persistence length l_{OSF} as given by eq C3 breaks down, as explained by Joanny and Barrat.[39] Still, the electrostatic repulsion between polymer segments can

be relevant and give rise to a chain stiffening on larger length scales, as explained by Khokhlov[40] and confirmed by Gaussian variational methods.[41] To that end, one defines an effective line charge density of a linear array of electrostatic blobs with blob size $R_{el} \simeq (l_0 L_{el})^{1/2}$,

$$\tilde{\tau} \simeq \frac{\tau L_{el}}{R_{el}} = \tau \left(\frac{L_{el}}{l_0}\right)^{1/2} \tag{C4}$$

Combining eqs C4 and C3, we obtain the effective electrostatic persistence length for a string of crumpled blobs,

$$\tilde{l}_{OSF} \simeq \frac{l_B^{1/3} l_0^{-2/3} \tau^{2/3}}{\kappa^2} \tag{C5}$$

This electrostatic stiffening is only relevant for $\tilde{l}_{OSF} > R_{el}$, leading to the bound of validity of $\tau l_B > \kappa^{3/2} l_0 l_B^{1/2}$.

To summarize: There are three distinct regimes. In the persistent regime, for $l_B\tau > (l_B l_0)^{1/2}\kappa$ and $l_B\tau > (l_B/l_0)^{1/2}$, the polymer takes on a rodlike structure with an effective persistence length larger than the bare persistence length and given by the Odijk expression eq C3. In the Gaussian-persistent regime, for $l_B\tau < (l_B/l_0)^{1/2}$ and $\tau l_B > \kappa^{3/2} l_0 l_B^{1/2}$, the polymer consists of a linear array of Gaussian electrostatic blobs, with an effective persistence length larger than the electrostatic blob size and given by eq C5. Finally, in the Gaussian regime, for $\tau l_B < \kappa^{3/2} l_0 l_B^{1/2}$ and $l_B\tau < (l_B l_0)^{1/2}\kappa$, the electrostatic repulsion does not lead to stiffening effects at any length scale.

References and Notes

(1) Oosawa, F. *Polyelectrolytes*; Dekker: New York, 1971.
(2) Dautzenberg, H.; Jaeger, W.; Kötz, B. P. J.; Seidel, C.; Stscherbina D. *Polyelectrolytes: Formation, characterization and application*; Hanser Publishers: Munich, Vienna, New York, 1994.
(3) Förster, S.; Schmidt, M. *Adv. Polym. Sci.* **1995**, *120*, 50.
(4) Barrat, J.-L.; Joanny, J.-F. *Adv. Chem. Phys.* **1996**, *94*, 1.
(5) Cohen Stuart, M. A. *J. Phys. Fr.* **1988**, *49*, 1001.
(6) Hoogeveen, N. G.; Cohen Stuart, M. A.; Fleer, G. J. *J. Coll. Interface Sci.* **1996**, *182*, 133; **1996**, *182*, 146.
(7) Mashl, R. J.; Grønbech-Jensen, N.; Fitzsimmons, M. R.; Lütt, M.; DeQuan, L. *J. Chem. Phys.* **1999**, *110*, 2219.
(8) Fang, Y.; Yang, J. *J. Phys. Chem. B* **1997**, *101*, 441.
(9) Rädler, J. O.; Koltover, I.; Salditt, T.; Safinya, C. R. *Science* **1997**, *275*, 810; Salditt, T.; Koltover, I.; Rädler, J. O.; Safinya, C. R. *Phys. Rev. Lett.* **1997**, *79*, 2582.
(10) Maier, B.; Rädler, J. O. *Phys. Rev. Lett.* **1999**, *82*, 1911.
(11) von Berlepsch, H.; Burger, C.; Dautzenberg, H. *Phys. Rev. E* **1998**, *58*, 7549.
(12) de Meijere, K.; Brezesinski, G.; Möhwald, H. *Macromolecules* **1997**, *30*, 2337.
(13) Miyano, K.; Asano, K.; Shimomura, M. *Langmuir* **1991**, *7*, 444.
(14) Bruinsma, R.; Mashl, J. *Europhys. Lett.* **1998**, *41*, 165. Bruinsma, R. *Eur. Phys. J. B* **1998**, *4*, 75.
(15) O'Hern, C. S.; Lubensky, T. C. *Phys. Rev. Lett.* **1998**, *80*, 4345.
(16) Decher, G.; Hong, J.-D.; Schmitt, J. *Thin Solid Films* **1994**, *210/211*, 831. v. Klitzing, R.; Möhwald, H. *Langmuir* **1995**, *11*, 3554. v. Klitzing, R.; Möhwald, H. *Macromolecules* **1996**, *29*, 6901.
(17) Decher, G. *Science* **1997**, *277*, 1232. Lösche, M.; Schmitt, J.; Decher, G.; Bouwman, W. G.; Kjaer, K. *Macromolecules* **1998**, *31*, 8893.
(18) Donath, E.; Sukhorukov, G. B.; Caruso, F.; Davis, S. A.; Möhwald, H. *Angew. Chem., Int. Ed. Engl.* **1998**, *16*, 37. Sukhorukov, G. B.; Donath, E.; Davis, S. A.; Lichtenfeld, H.; Caruso, F.; Popov, V. I.; Möhwald, H. *Polym. Adv. Technol.* **1998**, *9*, 759.
(19) Caruso, F.; Caruso, R. A.; Möhwald, H. *Science* **1998**, *282*, 1111. Caruso, F.; Niikura, K.; Furlong, D. N.; Okahata, Y. *Langmuir* **1997**, *13*, 3422.
(20) Papenhuijzen, J.; van der Schee, H. A.; Fleer, G. J. *J. Colloid Interface Sci.* **1985**, *104*, 540. Papenhuijzen, J.; Fleer, G. J.; Bijsterbosch, B. H. *J. Colloid Interface Sci.* **1985**, *104*, 553.
(21) Evers, O. A.; Fleer, G. J.; Scheutjens, J. M. H. M.; Lyklema, J. *J. Colloid Interface Sci.* **1986**, *111*, 446.
(22) van de Steeg, H. G. M.; Cohen Stuart, M. A.; de Keizer, A.; Bijsterbosch, B. H. *Langmuir* **1992**, *8*, 2538.
(23) Muthukumar, M. *J. Chem. Phys.* **1987**, *86*, 7230.
(24) Varoqui, R.; Johner, A.; Elaisari, A. *J. Chem. Phys.* **1991**, *94*, 6873. Varoqui, R. *J. Phys. II Fr.* **1993**, *3*, 1097.
(25) Borukhov, I.; Andelman, D.; Orland, H. *Europhys. Lett.* **1995**, *32*, 499. *Macromolecules* **1998**, *31*, 1665.
(26) Chatellier, X.; Joanny, J.-F. *J. Phys. II Fr.* **1996**, *6*, 1669.
(27) Joanny, J.-F. *Eur. Phys. J. B* **1999**, *9*, 117.
(28) Park, S. Y.; Bruinsma, R.; Gelbart, W. *Europhys. Lett.* **1999**, *46*, 454.
(29) Borisov, O. V.; Zhulina, E. B.; Birshtein, T. M. *J. Phys. II Fr.* **1994**, *4*, 913.
(30) Odijk, T. *Macromolecules* **1983**, *16*, 1340; **1984**, *17*, 502.
(31) Maggs, A. C.; Huse, D. A.; Leibler, S. *Europhys. Lett.* **1989**, *8*, 615.
(32) Gompper, G.; Burkhardt, T. W. *Phys. Rev. A* **1989**, *40*, 6124. Gompper, G.; Seifert, U. *J. Phys. A* **1990**, *23*, L1161.
(33) Bundschuh, R.; Lipowsky, R. To be published.
(34) The location of the continuous desorption transition in the parameter space and also its universal behavior can be exactly inferred from the ground-state scaling of the diffusion equation governing the polymer probability distribution and agrees up to numerical prefactors with the scaling result of eq 7. This is possible because at the continuous desorption transition the width of the polymer layer diverges and thus the semiflexible model can be asymptotically mapped on a flexible polymer model with a Kuhn length $a = 2l_{eff}$. The behavior of the layer thickness of a flexible polymer in the limit of strong confinement, eq 6, also follows by the same methods because the electrostatic potential in this limit is like a linear potential, for which the analysis can be done exactly.
(35) Dan, N. *Biophys. J.* **1996**, *71*, 1267; **1997**, *73*, 1842.
(36) Netz, R. R. *Phys. Rev. E* **1999**, *60*, 3174.
(37) Barrat, J.-L.; Joanny, J.-F. *J. Phys. II Fr.* **1994**, *4*, 1089.
(38) Andelman, D.; Brochard, F.; Joanny, J.-F. *J. Chem. Phys.* **1987**, *86*, 3673.
(39) Barrat, J.-L.; Joanny, J.-F. *Europhys. Lett.* **1993**, *24*, 333.
(40) Khokhlov, A. R.; Khachaturian, K. A. *Polymer* **1982**, *23*, 1742.
(41) Netz, R. R.; Orland, H. *Eur. Phys. J. B* **1999**, *8*, 81.

MA990263H